RSC Advances

PAPER

View Article Online
View Journal | View Issue

Cite this: *RSC Adv.*, 2021, **11**, 36564

Photo-triggered cargo release from liposome chlorin e6-bearing pullulan hybrid nanoparticles *via* membrane permeabilization†

Riku Kawasaki, ‡*[a] Reo Ohdake,‡[a] Takuro Eto,[a] Keita Yamana,[a] Toshimi Nakaya,[b] Takenori Ishida,[c] Akio Kuroda[c] and Atsushi Ikeda *[a]

Received 22nd October 2021
Accepted 8th November 2021

DOI: 10.1039/d1ra07807k

rsc.li/rsc-advances

A liposome chlorin e6-bearing pullulan nanogel hybrid was prepared as a light-triggered payload release platform. The current system enabled manipulation of the release profile of model drugs encapsulated by liposomes. Gelatin hydrogels that comprised hybrid nanoparticles could successfully control the delivery of cargo molecules to human mesenchymal stem cells with light stimuli without injury to the cells.

Introduction

Liposomes have been widely investigated as drug delivery carriers because of their excellent biocompatibility and ability to deliver cargo molecules.[1] Their value has been demonstrated both in fundamental research and also in the clinical application of several drug therapies for conditions such as cancer[2] and infections.[3] Despite their great promise as pharmaceutical agents, the mechanism of cargo release in clinically approved liposomal drugs involves the breakdown of nanocarriers, an approach that is not ideal for drug targeting and release with high specificity.[4] After the identification of the enhanced permeation and retention effect, that is nanomaterials tend to accumulate tumor tissue,[5] drug delivery systems using nanomaterials have been widely studied.[6] To establish nanoplatforms for targeted drug delivery, strategies based on the modification of ligand molecules[7] and/or the remote control of drug carriers[8] have been applied. Various internal and external signals, including heat,[9] light,[10] pH,[11] and specific enzymes,[12] have been used to trigger their functions. The use of optical stimuli is especially attractive because it can be applied with excellent spatial and temporal precision. Visible light (>600 nm) and near-infrared red light[13] can penetrate deeply into tissue and their application has been demonstrated *in vivo*.

Reactive oxygen species (ROS) can be generated and absorbed in the region between visible light and near-infrared red light, so photosensitizers (PSs) have been applied as the trigger for payload release.[14] The ROS generated by excited PSs leads to the oxidation of unsaturated bonds in phospholipids such as 1,2-dioleoyl-*sn*-glycero-3-phosphocholine (DOPC), resulting in payload release *via* chain disruption and collapse of the liposomal membrane.[15] Light triggers are therefore promising candidates for the achievement of controlled spatiotemporal release.

To manipulate this controlled release and targeting properties in liposomes, surface modification strategies have been applied, using stimulus-responsive polymers such as thermoresponsive[16] and pH-responsive polymers.[17] The modification of functional nanomaterials on the surface of liposomes has also been developed.[18] The introduced nanoparticles are able to work not only as stimulus-responsive units but also as delivery carriers. Self-assembled nanogels comprised cholesterol-bearing pullulan, and its derivatives have been introduced onto the surface of liposomes mainly *via* hydrophobic interactions, resulting in hydrophobic cholesteryl groups being anchored in the lipid bilayer.[19] Strategies based on supramolecular chemistry are attractive in the formulation of hybrid nanoparticles, because of their ease of use.

In this study, we report the development and implementation of a facile light-triggered cargo release system using liposome chlorin e6-bearing pullulan nanogel hybrid nanoparticles (Fig. 1).

We developed a chlorin e6-bearing pullulan (Che6P) nanogel as a photo-responsive building block.[20] The nanogel exhibited excellent photodynamic activity *in vitro via* photoirradiation at a specific wavelength. We used the system to form a hybrid nanoparticle with liposomes producing a photo-triggered controlled release system.

Results and discussion

Characterization of Che6P nanogel/liposome hybrid system

We developed a chlorin e6-bearing pullulan (Che6P) nanogel as a photo-responsive building block.[20] The nanogel exhibited

[a]*Program of Applied Chemistry, Graduate School of Advanced Science and Engineering, Hiroshima University, 1-4-1 Kagamiyama, Higashi Hiroshima, 739-8527, Japan. E-mail: riku0528@hiroshima-u.ac.jp; aikeda@hiroshima-u.ac.jp*

[b]*Digital Monozukuri (Manufacturing) Education and Research Center, Hiroshima University, 3-10-32 Kagamiyama, Higashi-Hiroshima, 739-0046, Japan*

[c]*Program for Biotechnology, Graduate School of Integrated Science for Life, Hiroshima University, 1-3-1 Kagamiyama, Higashi-Hiroshima, 739-8530, Japan*

† Electronic supplementary information (ESI) available: Experimental procedure and analytical data. See DOI: 10.1039/d1ra07807k

‡ These authors contributed equally to this work.

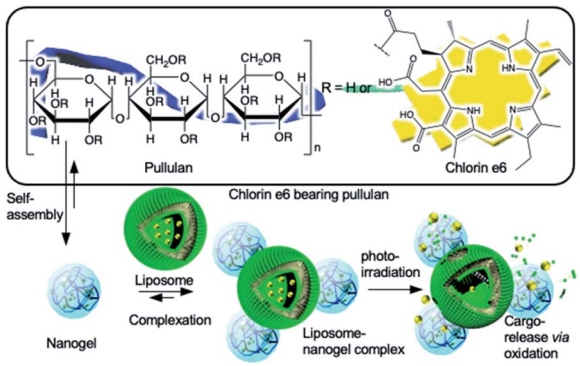

Fig. 1 Schematic illustration of formulation of liposome nanogel hybrid nanoparticles and photoirradiation-triggered payload release from liposome *via* membrane permeabilization.

excellent photodynamic activity *in vitro via* photoirradiation at a specific wavelength. We used the system to form a hybrid nanoparticle with liposomes producing a photo-triggered controlled release system.

Che6P nanogels were prepared by an established method, as previously reported.[21] Briefly, a dispersion of Che6P in MilliQ water was treated with a probe-type sonicator, resulting in the formation of a Che6P nanogel with a diameter of 100 nm, mainly *via* hydrophobic interactions. Their electrically negative character (−11 mV) was revealed by ζ-potential measurement. To form hybrid nanoparticles, Che6P nanogels were mixed with liposomes composed of 1,2-dioleyl-*sn*-glycero-3-phosphocholine (DOPC, Fig. S1a†) as an unsaturated phospholipid. After the complexation of Che6P nanogels with DOPC liposomes (hydrodynamic diameter, 80 nm; ζ-potential, −10 mV), dynamic light scattering was measured to evaluate the changes in hydrodynamic diameter produced by complexation. As shown in Fig. S2a,† the hydrodynamic diameter of the DOPC liposomes was increased by complexation. As the amount of Che6P nanogels co-incubated with liposomes increased, the hydrodynamic diameter of the hybrid decreased. The size changes reached a plateau when the DOPC liposomes reached a concentration of 0.5 mM. The interaction between the Che6P nanogels and the DOPC liposomes was estimated by measuring the ζ-potential (Fig. S3a†). After complexation at 0.5 and 1 mM, the ζ-potential of the DOPC liposome–Che6P nanogel hybrid reached −11 mV, suggesting that the DOPC was efficiently coated with electrically negative Che6P nanogels. To enhance the electrostatic interactions between the liposomes and the Che6P nanogels, we further examined the use of cationic liposomes (hydrodynamic diameter, 80 nm; ζ-potential, +37 mV) composed of cationic lipid (Fig. S1b†). Trends similar to those in DOPC liposomes were found in cationic liposomes containing 5% cationic lipid (Fig. S2b and S3b†). We further examined the interactions between the Che6P nanogels and liposomes by Förester resonance energy transfer (FRET) using fluorescently labeled liposomes containing NBD-1,2-dioleoyl-*sn*-glycero-3-phosphoethanolamine (NBD-PE). These energy transfer between two fluorophores are found when these fluorescent molecules located within 2 nm. Therefore, FRET occurred in case of nanomaterials only when the nanoparticles form the complex.[22] After complexation with liposomes containing NBD-PE, the FRET between the NBD and chlorin e6 were found in both DOPC liposomes and cationic liposomes, indicating that Che6P nanogels and liposomes were closely located (Fig. S4†). These results strongly support the contention that Che6P nanogels and liposomes formed hybrid nanoparticles. The complexation of DOPC liposomes with Che6P nanogels was further evaluated using fluorescence correlation spectroscopy (FCS).[23] FCS measures the diffusion time of a fluorescent molecule. The apparent diffusion time of a fluorescent molecule increases when the fluorescent molecule forms hybrid nanoparticles. The diffusion time of the Che6P nanogels in the presence of DOPC liposomes was larger than that of the Che6P nanogels alone (Fig. 2a). The correlation curve could be fitted by a single-component equation, indicating that all of the Che6P nanogels formed hybrid nanoparticles with DOPC liposomes.

We next conducted a morphological observation of the liposome–Che6P nanogel hybrid using transmission electron microscopy. The Che6P nanogels were attached to the surface of the DOPC liposomes one by one or one by two (Fig. 2b and S5†). Similar hybrid nanoparticles were observed in the case of cationic liposomes (Fig. S6†). To evaluate the effect of the complexation of liposomes with Che6P on the phase transition for DOPC, we performed a differential scanning calorimetry measurement of the DOPC liposome–Che6P nanogel hybrid. For the DOPC liposome/Che6P nanogel hybrid, the phase transition of DOPC shifted to a higher temperature, as did that of the DOPC containing chlorin e6 system (Fig. 2c), indicating that Che6 molecules in Che6P nanogels anchored into the lipid bilayer of the DOPC liposomes.[24] Phase transition shifts were also observed in cationic liposomes (Fig. S7†). The peak shift in the phase transition of DOPC in DOPC liposome–Che6P nanogel hybrids was larger than that of cationic liposome–Che6P nanogel hybrids. These differences imply that the formulation of hybrid nanoparticles with DOPC is mainly *via* hydrophobic interactions, which result in the anchoring of the chlorin e6 molecules into the lipid membrane. By contrast, large parts of the chlorin e6 molecules were bound to the surface of cationic liposomes by the formation of hybrids mainly *via* electrostatic interactions. All these results support our hypothesis that Che6P nanogels form hybrid nanoparticles with liposomes mainly *via* the anchoring of their Che6 molecules into the lipid bilayer. To visualize the surface modifications of the Che6P nanogel on liposomes, we applied fluorescently labeled giant liposomes coated on silica microparticles (GUVs). GUVs containing NBD-PE formed spontaneously when liposomes and silica microparticles were mixed (Fig. S8a and b†).[25] When the GUVs were incubated with Che6P nanogels, confocal laser scanning microscopy revealed that fluorescence signals from the Che6P nanogels and lipids overlapped (Fig. S8c and d†), indicating that Che6P nanogels were introduced on the surface of the GUVs.

Photo-triggered payload release

We next evaluated the capability to generate singlet oxygen *via* photoirradiation using 9,10-anthracenediyl-bis(methylene)

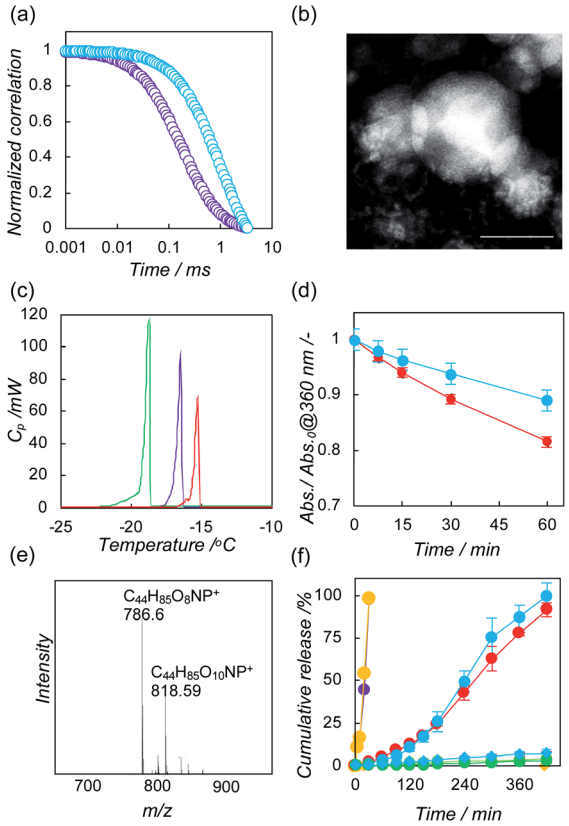

Fig. 2 Characterization of liposome–Che6P nanogel hybrid nanoparticle. (a) Normalized correlation curve of Che6P nanogel (purple) and hybrid (blue). (b) Representative morphological images of hybrids. Samples were stained with 1% phosphotungstic acid. The complex was observed with transmission electron microscope. (c) DSC thermograms showing the effect of Che6P nanogels on the phase transition for DOPC liposome. (DOPC liposome, green; DOPC liposome/Che6P nanogel hybrid, purple; DOPC liposome containing chlorin e6, red). (d) Singlet oxygen generation capacity of hybrids. Time course in bleaching 9,10-anthracenediyl-bis(methylene)-dimalonic acid (ABDA) *via* oxidation by singlet oxygen (DOPC, blue; cationic lipid; red), (Che6P, 100 μg mL^{-1}; lipid, 100 μM; ABDA, 25 μM). (e) ESI-MS spectrum of DOPC after photoirradiation. Peak appearing at *m/z* value of 786 and 818 corresponded to DOPC ($C_{44}H_{85}O_8NP^+$) and oxidized DOPC ($C_{44}H_{85}O_{10}NP^+$), respectively. (f) Cumulative payload release *via* photoirradiation. Che6P nanogel–DOPC hybrid (blue: Che6P, 100 μg mL^{-1}; DOPC, 100 μM, yellow: Che6P, 1 mg mL^{-1}; DOPC, 100 μM). Che6P nanogel–cationic liposome hybrid (red: Che6P, 100 μg mL^{-1}; lipid, 100 μM, purple: Che6P, 1 mg mL^{-1}; lipid, 100 μM). DOPC liposome, green; cationic liposome, deep blue). Circle symbol and diamond symbol indicate with irradiation group and without irradiation group, respectively.

dimalonic acid (ABDA).[26] The absorption of ABDA is quenched *via* oxidation with singlet oxygen (Scheme S1†). During irradiation with light at 600–800 nm, ABDA was gradually consumed by singlet oxygen generated by liposome–Che6P nanogel hybrids and cationic liposome–Che6P nanogel hybrids (Fig. S9†). After 60 min of irradiation, DOPC liposome–Che6P nanogel hybrids consumed 10% of ABDA and cationic liposome–Che6P nanogel hybrids consumed 20% of ABDA (Fig. 2d). These differences in singlet oxygen generation capacity may be caused by the dissociation degrees of chlorin e6 because complexation for self-associated PS generally lessens their photodynamic activity.[9] To address the association of chlorin e6, we conducted UV-Vis absorption spectrum measurement and fluorescence spectrum measurement. After the complexation of Che6P nanogels with liposomes, the UV-Vis spectra derived from chlorin e6 were sharper, indicating that the interaction with liposomes causes the dissociation of chlorin e6 in Che6P nanogels (Fig. S10†). In cationic liposomes, the changes in UV-Vis spectra were more efficiently induced than in DOPC liposomes.

Fluorescence from chlorin e6 was recovered following complexation with liposomes. Stronger fluorescent signals were detected in cationic liposome–Che6P nanogel hybrids compared to DOPC liposome–Che6P nanogel hybrids (Fig. S11†). These results also support our hypothesis that the self-associated chlorin was partially dissociated by anchoring the hydrophobic chlorin e6 in the liposomal membrane. This feature is ideal for achieving efficient photo-triggered release using current systems *via* the oxidation of phospholipids due to closing effects. Using electrospray ionization mass spectroscopy, oxidized lipids were found from DOPC liposome–Che6P nanogel hybrids after photoirradiation (Fig. 2e), suggesting that the oxidization of DOPC produces peroxide and/or epoxide derivatives (Fig. S12†).[15]

We demonstrated the photo-triggered payload release properties of liposome–Che6P nanogel hybrids using a model fluorescent drug, calcein (Che6P, 0.1 mg mL^{-1}; lipid, 0.1 mM).[27] The fluorescence from calcein incorporated into the hydrophilic core of liposomes is self-quenched, and their fluorescence is recovered following release from liposomes. Under dark conditions, no release of calcein was found in either hybrid system (Fig. 2f, diamond symbols). Calcein-loaded liposomes did not release their cargo in the absence of Che6P nanogels.

However, encapsulated calcein was gradually released from liposome–Che6P nanogel hybrids by photoirradiation (Fig. 2f, circle symbols), indicating that the current system using liposome–Che6P nanogel hybrids is able to work as a photo-triggered payload release system. After 7 h of irradiation, almost all the calcein was released from the liposomes, and there were no significant differences in the release profiles between the DOPC liposome–Che6P nanogel hybrids and cationic liposome–Che6P nanogel hybrids. More than 80% of chlorin e6 was not bleached *via* photoirradiation (Fig. S13†). To control the release profile *via* photo-irradiation, the amount of Che6P against liposome increased (Che6P, 1 mg mL^{-1}; lipid, 0.1 mM). As a result, the release of cargo was accelerated with increasing Che6P nanogels (Fig. 2f, yellow and purple symbols). The release of cargo started within 5 min and all the calcein was released within 30 min. These results suggesting release profiles can be tuned by varying the ratio of Che6P nanogel against liposome. The number of liposome–Che6P nanogel hybrids also decreased over time (Fig. S14†), suggesting that the scattering intensity from liposome–Che6P nanogel hybrids was lessened by the collapse of liposomes. These results support the contention that the release of the cargo was induced by the collapse of the liposomal membrane *via* the oxidation of lipids.

Photo-triggered payload release from hydrogel comprising of hybrid nanoparticles

To address the value of the nanogel hybrids for regenerative medicine, we further examined payload release *via* photo-induced oxidization using DOPC–Che6P nanogel hybrids immobilized in gelatin hydrogels.[28,29] Construction of binary systems immersed in hydrogels are advantageous to lessen oxidative stress from leaked photosensitizer by control the pharmacokinetics of the hybrid nanoparticles by fixation of hybrid nanoparticles in the hydrogel. Initially, we confirmed release of Che6 molecules from the hydrogel (Fig. S15†). In case with Che6P nanogel/DOPC liposome hybrid containing hydrogel, Che6 molecule was not released from the hydrogels. In contrast, Che6 molecules are gradually released from the hydrogel in case of Che6P molecule containing DOPC liposome.

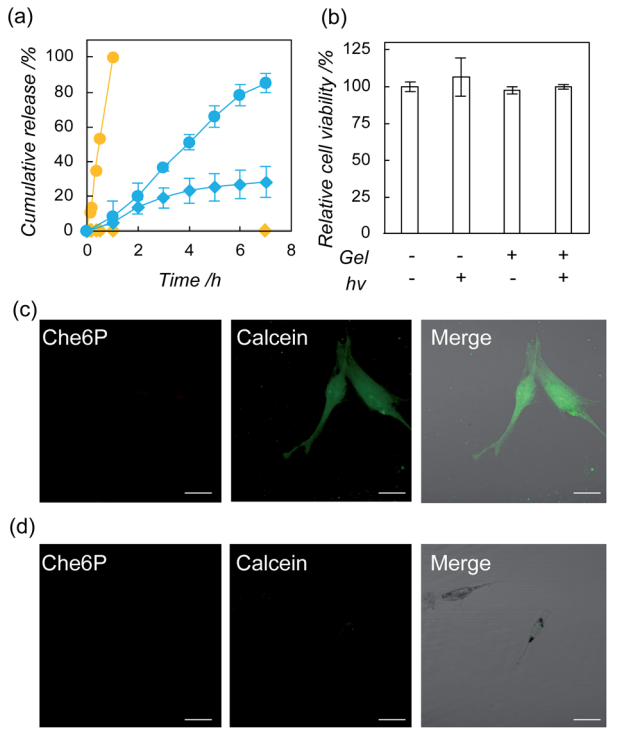

Fig. 3 (a) Photo-triggered payload release from DOPC liposome–Che6P nanogel hybrid immobilized hydrogel (circle, with irradiation; diamond, without irradiation) (blue; Che6P, 0.1 mg mL^{-1}; DOPC, 0.1 mM: yellow; Che6P, 1 mg mL^{-1}; DOPC, 0.1 mM). (b) Effects of photoirradiation and DOPC liposome–Che6P nanogel hybrid immobilized hydrogel on cell viability of human mesenchymal stem cell (hMSC). The cells were exposed to the hydrogel for 24 h and photoirradiation was carried out for 6 h. The cell viability was evaluated by cell counting kit-8. ($N = 3$). (c) Cellular uptake of Che6P nanogel (red) and calcein with irradiation. The cells were co-incubated with hydrogel containing DOPC liposome/Che6P nanogel hybrid for 24 h and cellular uptake was confirmed by confocal laser scanning microscopy. Scale bar represents 10 μm. (d) Cellular uptake of Che6P nanogel (red) and calcein with irradiation. The cells were co-incubated without hydrogel containing DOPC liposome/Che6P nanogel hybrid. Photoirradiation was carried out in initial 6 h. After additional 18 h, the cells were observed by confocal laser scanning microscopy. Scale bar represents 10 μm.

The result is advantageous to attain controlled release without harmful injury from singlet oxygen generated by leaked Che6 molecules. We first investigated the release profile of the calcein from the hydrogel. After the preparation of the gelatin hydrogel containing DOPC–Che6P nanogel hybrids, the leakage of calcein was found, implying that the liposomes were partially collapsed during gelation. The rate of release of calcein from the hydrogels with photoirradiation was much higher than that without photoirradiation (Fig. 3a), and almost all the calcein was released from the hydrogel after 7 h. Furthermore, the release can be accelerated by increasing amount of Che6P nanogels (Che6P, 1 mg mL^{-1}; lipid, 0.1 mM) as release study. Finally, all the calcein was released within 30 min. We next investigated the effects of gelatin hydrogels containing DOPC–Che6P nanogels with photoirradiation on the viability of human mesenchymal stem cell (hMSC) using a modified MTT assay.[30] No apparent cytotoxicity was found in any group, indicating that the gelatin hydrogel containing DOPC–Che6P nanogels with photoirradiation did not affect the viability of hMSCs under current conditions (Fig. 3b). Finally, we used confocal laser scanning microscopy and flow cytometry to demonstrate the deliverability of cargo molecules from gelatin hydrogels containing DOPC–Che6P nanogel hybrid to hMSC *via* photoirradiation. As shown in Fig. 3c, strong fluorescence signals from calcein were detected in the cytosol in the presence of photoirradiation. By contrast, no fluorescence from calcein was found within cells in the absence of photoirradiation (Fig. 3d). In addition, 30 min irradiation was enough to deliver cargo molecules to MSC when ratio of Che6P nanogel increased against liposome (Fig. S16†). These results indicate that the current system could successfully deliver cargo molecules to cells by responding to light. No fluorescence signals from Che6P were detected within cells, suggesting that Che6P nanogels were still trapped in the gelatin hydrogel during photoirradiation. These results were highly similar to the results from flow cytometry (Fig. S17†).

Conclusions

In conclusion, the Che6P nanogel formed a stable hybrid with DOPC liposomes and cationic liposomes. By applying photoirradiation to this hybrid, liposomes released encapsulated cargo molecules *via* the oxidation of the lipids. Current systems functioned as a photo-triggered payload release platform in the gelatin hydrogels, and the hydrogel systems were able to deliver cargo molecules to hMSCs without injury. Our strategy has considerable potential for use in photo-triggered payload release platforms for regenerative medicine.

Author contributions

The manuscript was written through contribution of all the authors. All authors have given approval to the final version of the manuscript. R. K., R. O, and T. E. were mainly conducted all the experiments. K. Y. and T. N. carried out characterization studies including TEM observation and DSC measurement. T. I. and A. K supported cellular studies using MSCs.

Conflicts of interest

There are no conflicts to declare.

Acknowledgements

This work was supported by the Japan Society for the Promotion of Science, KAKENHI (R. K., JP19K15401), and Foundation from Kyoto Technology and Science Center (R. K.). Experiments using confocal laser scanning microscopy and transmission electron microscopy were conducted in Natural Science Center for Basic Research and Development, (N-BARD). We would like to express great appreciation to Prof. Kazunari Akiyoshi and Dr Yoshihiro Sasaki, Kyoto University, for their kind technical help and advice in fluorescence correlation spectroscopy.

Notes and references

1 B. S. Pattni, V. V. Chupin and V. P. Torchilin, *Chem. Rev.*, 2015, **115**, 10938–10966.
2 J. Zhang, X. Li and L. Huang, *Adv. Drug Delivery Rev.*, 2020, **154**, 245–273.
3 G. M. Jensen and D. F. Hodgson, *Adv. Drug Delivery Rev.*, 2020, **154–155**, 2–12.
4 E. Yuba, *J. Mater. Chem. B*, 2020, **8**, 1093–1107.
5 H. Maeda, J. Wu, T. Sawa, Y. Matumura and K. Hori, *J. Controlled Release*, 2000, **65**, 271–284.
6 K. W. Witwer and J. Wolfram, *Nat. Rev. Mater.*, 2021, **6**, 103–106.
7 M. Srinivasarao and P. S. Low, *Chem. Rev.*, 2017, **117**, 12133–12164.
8 N. Kamaly, B. Yameen and J. Wu, *Chem. Rev.*, 2016, **116**, 2602–2663.
9 R. Kawasaki, K. Yamana, R. Shimada, K. Sugikawa and A. Ikeda, *ACS Omega*, 2021, **6**, 3209–3217.
10 C. J. Carling, M. L. Viger, V. A. N. Huu, A. V. Garcia and A. Alumutairi, *Chem. Sci.*, 2015, **6**, 335–341.
11 A. Stubelius, W. Sheng, S. Lee, J. Olejniczak, M. Guma and A. Almutairi, *Small*, 2018, **14**, 1800703.
12 C. E. Callmann, C. V. Barback, M. P. Thompson, D. J. Hall, R. F. Mattrey and N. C. Gianneschi, *Adv. Mater.*, 2015, **27**, 4611–4615.
13 A. Y. Rwei, W. Wang and D. S. Kohane, *Nano Today*, 2015, **10**, 451–467.
14 P. Enzian, C. Schell, A. Link, C. Malich, R. Pries, B. Wollenberg and R. Rahmanzadeh, *Mol. Pharmaceutics*, 2020, **17**, 2779–2788.
15 I. O. L. Bacellar, M. S. Baptista, H. C. Junqueira, M. Wainwright, F. Thalmann, C. M. Marques and A. P Schroder, *Biochim. Biophys. Acta, Biomembr.*, 2018, **1860**, 2366–2373.
16 K. Kono, T. Ozawa, T. Yoshida, F. Ozaki, Y. Ishizaka, K. Maruyama, C. Kojima, A. Harada and S. Aoshima, *Biomaterials*, 2010, **31**, 7096–7105.
17 T. Nishimura, Y. Sasaki and K. Akiyoshi, *J. Am. Chem. Soc.*, 2020, **142**, 154–161.
18 E. Miyako, S. A. Chechetka, M. Doi, E. Yuba and K. Kono, *Angew. Chem., Int. Ed.*, 2015, **54**, 9903–9906.
19 Y. Sekine, Y. Moritani, T. I. Fukuzawa, Y. Sasaki and K. Akiyoshi, *Adv. Healthcare Mater.*, 2012, **1**, 722–728.
20 R. Kawasaki, R. Ohdake, K. Yamana, T. Eto, K. Sugikawa and A. Ikeda, *J. Mater. Chem. B*, 2021, **9**, 6357–6363.
21 S. Sawada, Y. Sato, R. Kawasaki, J. Yasuoka, R. Mizuta, Y. Sasaki and K. Akiyoshi, *Biomater. Sci.*, 2020, **8**, 619–630.
22 J. Shi, F. Tian, J. Lyu and M. Yang, *J. Mater. Chem. B*, 2015, **3**, 6989–7005.
23 S. Takeda, T. Nishimura, K. Umezaki, A. Kubo, M. Yanase, S. Sawada, Y. Sasaki and K. Akiyoshi, *Biomater. Sci.*, 2019, **7**, 1617–1622.
24 M. Bolean, A. M. S. Simao, B. Z. Favarin and P. Ciancaglini, *Biophys. Chem.*, 2010, **152**, 74–79.
25 A. E. LaBauve, T. E. Rinker, A. Noureddine, R. E. Serda, J. Y. Howe, M. B. Sherman, A. Rasley, C. J. Brinker, D. Y. Sasaki and O. A. Negrete, *Sci. Rep.*, 2018, **8**, 13990.
26 T. Entradas, S. Waldron and M. Volk, *J. Photochem. Photobiol., B*, 2020, **204**, 111787.
27 Y. Yang, X. Liu, W. Ma, Q. Xu, G. Chen, Y. Wang, H. Xiao, N. Li, X. Li. Liang, M. Yu and Z. Yu, *Biomaterials*, 2021, **265**, 120456.
28 Y. Ikada and Y. Tabata, *Adv. Drug Delivery Rev.*, 1998, **31**, 287–301.
29 S. Grijalvo, J. Mayr, R. Eritja and D. D. Diaz, *Biomater. Sci.*, 2016, **4**, 555–574.
30 H. Tominaga, M. Ishiyama, F. Ohseto, K. Sasamoto, T. Hamamoto, K. Suzuki and M. Watanabe, *Anal. Chem.*, 1999, **36**, 47–50.